Studies on erythrocytes in malaria infected blood sample with Raman optical tweezers

Raktim Dasgupta
Ravi Shanker Verma
Sunita Ahlawat
Abha Uppal
Pradeep Kumar Gupta

Studies on erythrocytes in malaria infected blood sample with Raman optical tweezers

Raktim Dasgupta, Ravi Shanker Verma, Sunita Ahlawat, Abha Uppal, and Pradeep Kumar Gupta
Raja Ramanna Centre for Advanced Technology, Laser Biomedical Applications and Instrumentation Division, Indore-452013, India

Abstract. Raman spectroscopy was performed on optically trapped red blood cells (RBCs) from blood samples of healthy volunteers (h-RBCs) and from patients suffering from *P. vivax* infection (m-RBCs). A significant fraction of m-RBCs produced Raman spectra with altered characteristics relative to h-RBCs. The observed spectral changes suggest a reduced oxygen-affinity or right shifting of the oxygen-dissociation curve for the intracellular hemoglobin in a significant fraction of m-RBCs with respect to its normal functional state. © *2011 Society of Photo-Optical Instrumentation Engineers (SPIE)*. [DOI: 10.1117/1.3600011]

1 Introduction

Malaria is often associated with the development of a severe anemic condition in patients, which causes more than half of the mortality resulting from the disease.[1] The pathogenesis of malarial anemia is complex and not well understood. Since the destruction of the parasitized red blood cells (p-RBCs) can only account for less than 10% of the overall red blood cell (RBC) loss in malaria patients,[2,3] the accelerated destruction of the nonparasitized RBCs (np-RBCs) is believed to be the primary cause behind development of the severe anemic condition in patients. The reduced deformability of np-RBCs,[4–12] which may lead to failure in passing through splenic clearance or phagocytosis by spleen cells due to biochemical changes induced by parasite metabolites,[2] are some of the factors that could trigger early removal of np-RBCs in malaria patients. Apart from the accelerated destruction of np-RBCs, other factors like dyserythropoiesis or ineffective erythropoiesis, reduced hemoglobin-oxygen affinity or disturbed metabolic pathways in RBCs may also contribute to the development of malarial anemia and the associated hypoxia condition. Further studies on np-RBCs are therefore required to get answers to these questions.

Spectroscopic techniques and in particular Raman scattering has been found to be useful for investigating RBCs in malaria infected blood samples. For example, the use of confocal Raman spectroscopy could shed new lights on the electronic structure of hemozoin, a by-product of hemoglobin (Hb) catabolization by the malaria parasite and also an important target site for anti-malarial drugs.[13,14] Significant differences in Raman spectra have been reported for p-RBC and np-RBC in continuous *in-vitro* culture.[15,16] Therefore, Raman spectroscopy may help in understanding the altered properties of RBCs in malaria patients (m-RBCs). Raman optical tweezers[17,18] are particularly appropriate for probing subtle changes in m-RBCs as acquisition of Raman spectrum from RBC optically trapped in buffer media helps avoid perturbations arising due to the immobilization of the cells on substrate.[19] Further, as optical tweezers can trap objects away from cover glass surface, background from the substrate/immersion medium can be effectively reduced compared to typical Raman micro-spectroscopy measurements leading to an improvement in the signal to noise ratio (SNR) of the Raman spectra.

Here, we report a Raman spectroscopy study of m-RBCs collected from patients suffering from the *P. vivax* infection, using Raman optical tweezers. The results show marked differences in the Raman spectra of a significant fraction (∼30%) of m-RBCs relative to their normal counterpart (h-RBC). These changes are consistent with the possibility that the m-RBCs were incompletely oxygenated, even when they were kept in ambient oxygen, i.e., an excess of oxygen.

2 Materials and Methods

A schematic of the experimental set-up is shown in Fig. 1(a). The 785-nm cw beam from a Ti:Sapphire laser (Mira 900, Coherent Inc), pumped by a 532-nm diode pumped solid state laser (Verdi-5, Coherent Inc.), was used for both trapping the cells and exciting the Raman spectra. The use of a near infrared laser beam for trapping/excitation reduces the absorption-induced degradation of the RBCs and also helps minimize the fluorescence background. The laser beam was filtered to obtain a smooth profile [Fig. 1(b) and 1(c)] and then introduced into a home-built inverted microscope equipped with a high numerical aperture (NA) objective lens (Olympus 60×, NA 1.42), forming an optical trap. For trapping and acquisition of Raman spectra, we used a laser power of ∼2 mW at the specimen plane. The laser spot size at the focus was ∼1 μm and the RBCs were trapped ∼15 μm above the bottom cover plate of the sample holder. A holographic notch filter (notch filter 1), was used to reflect the 785-nm trapping/excitation beam, which was incident on it at an angle of ∼12 deg. The Raman signal backscattered from the trapped

Address all correspondence to: Raktim Dasgupta, Raja Ramanna Centre For Advanced Technology, Block-D, Indore, Madhya Pradesh 452013 India. Tel: 917312488427; Fax: 917312488425; E-mail: raktim@rrcat.gov.in.
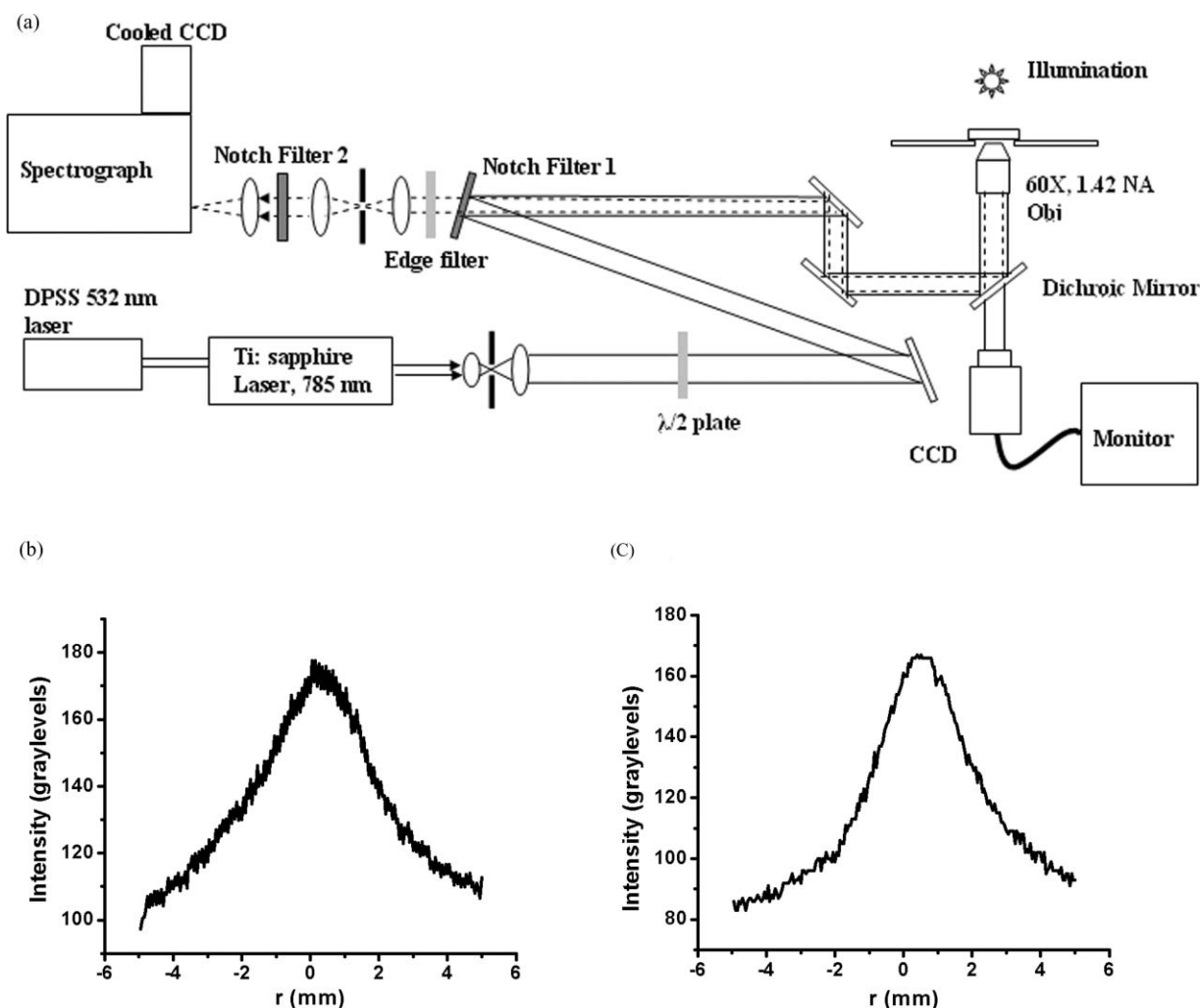
Fig. 1 (a) Experimental set-up. The solid line shows the trapping/excitation beam, whereas the dotted line indicates the Raman signal. For removing high-frequency noise from the laser beam profile, a spatial filter assembly consisting of a pair of convex lenses having 50- and 300-mm focal length and a 50-μm diameter pinhole placed at the focal point of the first lens was used. (b) Original beam profile and (c) the beam profile after spatial filtering, as measured using a monochrome CCD camera.

RBC was collimated by the objective lens and passed back along the same optical pathway. The notch filter 1 transmits the Raman signals above 800 nm, which are then passed through a 100-μm confocal pinhole to reject most of the off-focus Rayleigh scattered light. It was thereafter passed through another notch filter (notch filter 2) that further removes the Rayleigh-scattered laser light. The beam was then focused onto the entrance slit of an imaging spectrograph (Shamrock SR-303i, Andor Technology plc). The spectrograph was equipped with either a 600 lines/mm grating or a 1200 lines/mm grating blazed at an wavelength of 900 nm and incorporates a back-illuminated CCD (iDus DU420-BR-DD, Andor Technology plc) camera thermoelectrically cooled down to $-80\,^{\circ}$C. To allow for observation of the trapped RBC, a green-filtered halogen illumination source and a video CCD camera system were used.

Calibration of the spectrometer was performed using toluene (Spectroscopic grade, Aldrich) and the assignment of the peaks was made from standard spectra. The spectral resolution of our Raman system is about 6 cm^{-1} with 600 lines/mm grating and the Raman spectra can be recorded in the range from $\sim$500 to 2100 cm^{-1}. With 1200 lines/mm grating, the resolution is $\sim$4 cm^{-1} and spectra could be recorded in the range 950 to 1600 cm^{-1}. To remove the presence of the background from the RBC spectra, the background was acquired without a cell in the optical trap. This was subtracted from the original spectra to produce the Raman spectra of the trapped RBC. Further removal of the background could be obtained using the Lieber and Mahadevan-Jansen iterative polynomial fitting method[20] for better visualization of the spectra. It is pertinent to note that for all of the analysis presented in the paper, Raman spectra in the region 600 to 1700 cm^{-1} is used and an identical cropping window of 550 to 1750 cm^{-1} was used while applying the polynomial baseline fitting. This is done to ensure that nature of the fitted polynomials have minimal variation from spectra to spectra so that the position of zero is closely matched for all of the spectra. As will be discussed in Sec. 3, the spectral changes observed in our study were noted to be related to the oxy/deoxy conformational changes of heme from a planar to a nonplanar form. Therefore, to quantitatively compare the related spectral changes, we normalized the spectra with

respect to the phenylalanine band (1001 cm^{-1}). The choice of a phenylalanine band for the normalization was made because previous studies on the changes observed in Raman spectra of RBCs arising due to oxy-deoxy transitions[21–24] suggest that the changes in the Raman spectra are primarily in the bands arising due to heme as it undergoes significant conformational changes during the process. It is also pertinent to note here that the changes in the membrane of the malaria affected RBCs (Refs. 2, 4, 10, and 25) can also lead to changes in the intensity of the phenylalanine band. However, previous works suggest that the contribution of membrane proteins to the Raman bands of RBCs is minimum compared to the contribution from intracellular hemoglobin.[21–24] In view of this, it appears a reasonable assumption that the intensity of phenylalanine band can function as a normalizer. All of the measurements of the peak intensities of the Raman bands were carried out on the normalized spectra.

Blood (1 ml) was collected by venipuncture from healthy volunteers and malaria patients in glass tubes containing ethylenediaminetetraacetic acid ethylenediaminetetraacetic (5.4 mg/3 ml) as an anticoagulant. RBCs were separated from these anticoagulated blood samples by centrifugation at 3000 rpm for three minutes. The separated RBCs were then washed with phosphate buffer saline and suspended in 1.5-mM phosphate buffer containing 290-mM sucrose. This buffer maintains the osmolarity of the suspending media and inhibits the adherence of cells to glass surface.[26] The cell sample was kept in the open on a laminar flow table (which was earlier sterilized using UV radiation and chemical cleaning of the working surface) for about a one-hour period before recording their Raman spectra. Appropriate dilutions of the cells in buffer solution were then used for experiments.

Raman spectra were recorded from blood samples collected from five healthy donors and five patients suffering from the *P. vivax* infection. For the malaria samples investigated, the number of p-RBCs, as confirmed from acridine orange staining, was ∼1 to 2% of all cells (m-RBCs), and therefore, all of the RBCs studied from malaria infected samples were treated as np-RBC type. While for each blood sample collected from healthy donors, Raman spectra were recorded from ∼15 RBCs; for blood samples collected from malaria patients, Raman spectra were recorded from at least 50 cells in each sample. This was done to account for the much larger cell-to-cell spectral variations in the spectra of RBCs from blood samples of malaria patients.

3 Results and Discussions

In Fig. 2(A) we show the Raman spectra recorded between 600 and 1700 cm^{-1}, from h-RBCs held under optical trap ∼15 μm above the substrate. The excitation laser power and the acquisition time were ∼2 mW and ∼30 s, respectively. Curve (a) is the spectra recorded when the h-RBC was in the trap, (b) is the background with h-RBC removed from the trap region, and curve (c) is the background subtracted Raman spectrum, suitably magnified for viewing. In Fig. 2(B) we show the corresponding spectra from an h-RBC adhering on the glass substrate. In conformity with previous reports,[18,19] an improvement in SNR can be seen for the trapped cell over the fixed cell. For the spectra presented here, SNR is ∼16 dB for the fixed cell and ∼22 dB for the optically trapped cell.

There are several reports[21,22,27] on photoinduced changes in the Raman spectra of RBC. In the micro-Raman spectroscopic study carried out by Wood et al.[21] using the same laser wavelength and similar focusing geometry (spot diameter ∼1 to 2 micrometer), no photoinduced changes could be observed with 18 mW of laser power for exposure duration up to 200 s. We chose a laser power level of ∼2 mW over a time duration of 30 s that is much lower than the safe limit of exposure indicated in previous studies.[21,27] To further ensure authentic Raman spectra that is not influenced by photoinduced alterations, we carried out time lapsed measurements on the Raman spectra of RBCs at different power levels. The recorded time lapsed Raman spectrum at 2 mW of trap beam power over 30-second period is shown in Fig. 2(C). The time lapsed Raman spectra of trapped RBCs over a period of 30 s and with trapping power of ∼2 mW revealed no changes in the spectra or the background level, indicating absence of any photoinduced changes of the cells. This result is consistent with our estimate of the <1 °C rise in temperature of the cell for laser power of ∼2 mW based on the work of Peterman et al.[28] At 5 mW laser power, significant changes in the Raman spectra (like increase in the intensity of the Raman bands at 975, 1244, and 1366 cm^{-1} and the baseline offset and a decrease in the intensity of 1546 cm^{-1} band) were observed for exposure time of more than 70 s [Fig. 2(D)]. For 2 mW laser power, no changes were observed even for hundreds of seconds of exposure. Therefore, for all of the experiments reported in the manuscript, the laser power used was 2 mW and the exposure duration was kept limited to 30 s. Notably, the spectra presented in Fig. 2(D) were recorded with the 1200 lines/mm grating and therefore resulted in a slight wavenumber shift of the peaks compared to the spectra recorded using 600 limes/mm grating used in the rest of the experiments. Details of these studies have been presented in our earlier publication.[29] It is also pertinent to note that cells held under the optical trap can undergo some positional fluctuations, which was estimated to be <50 nm (<1% of cell diameter) for the trap conditions used in our studies. Since RBCs are fairly homogeneous structures, these small fluctuations in the cell position are not expected to contribute to significant changes in the Raman spectra. However, the use of low trap beam power results in poor SNR of spectra recorded from individual cells. To address this aspect, we collected spectra from about 100 cells and used the mean spectrum of each class of cells (h-RBCs or m-RBCs) that had much improved SNR for analysis.

To show the interclass variability of the Raman spectra of h-RBCs and m-RBCs, we show representative Raman spectra collected from five individual h-RBCs and m-RBCs in Figs. 3(a) and 3(b), respectively. The spectra of h-RBCs are similar and display fairly uniform peak distribution and intensities from one cell to another. However, for m-RBCs, large variability was observed. While the spectrum of the ∼70% of the m-RBCs was similar to that for h-RBCs, ∼30% of m-RBCs show a decrease in the intensity of the low spin (oxygenated-Hb) marker Raman band at 1223 cm^{-1} along with a concomitant increase in the high spin (deoxygenated-Hb) marker band at 1210 cm^{-1} present in the methine C-H deformation region. We designate the m-RBCs with Raman spectra similar to h-RBCs as nonmodified m-RBCs (nm-m-RBCs) and the other as modified m-RBCs (m-m-RBCs). The mean spectrum for h-RBCs, nm-m-RBCs, and m-m-RBCs averaged over all of the spectra collected
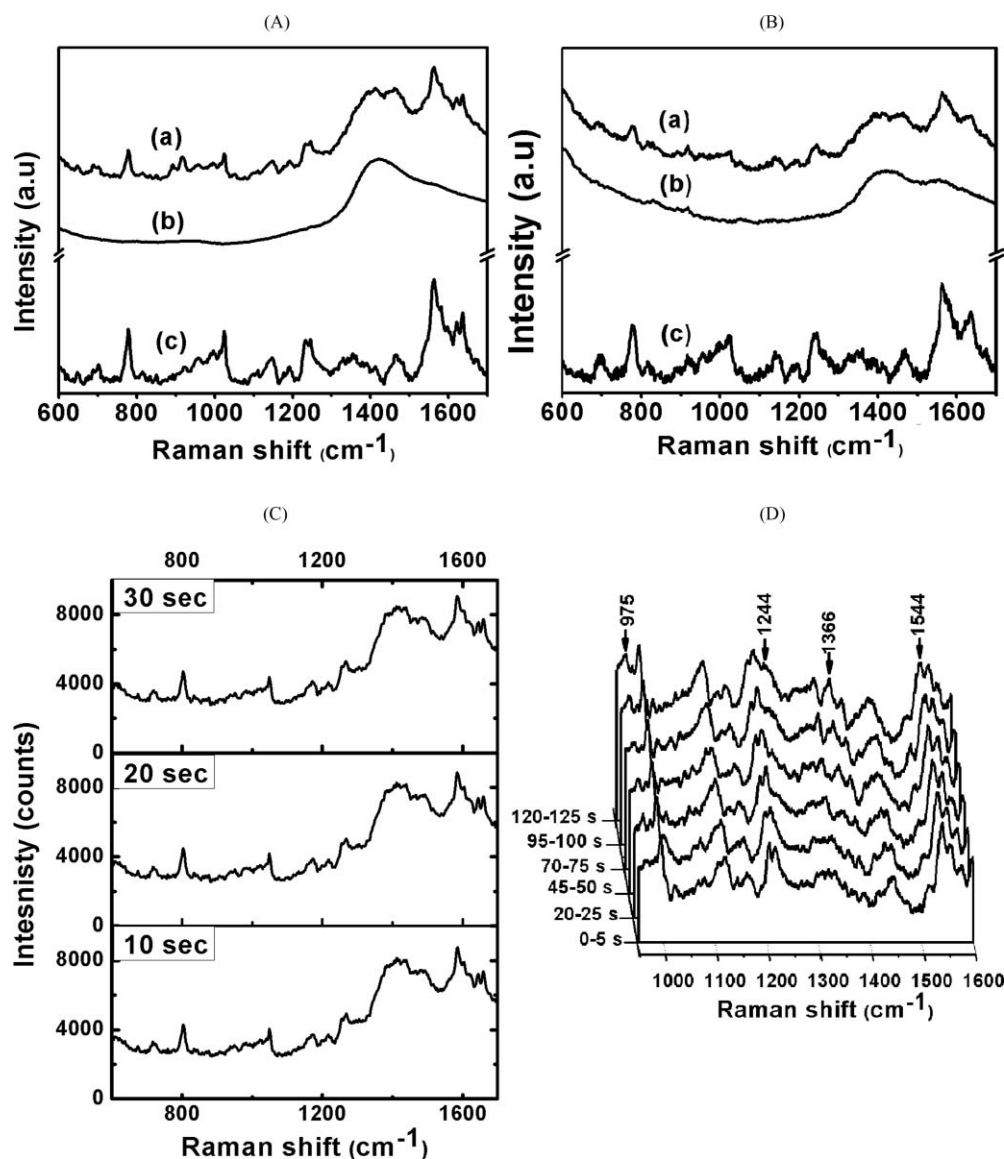
Fig. 2 (A) (a) Raman spectra of h-RBC optically trapped ~15 μm above the glass substrate, (b) is the background, and (c) is the subtraction between (a) and (b). (B) (a) Raman spectra of h-RBC adhered to the glass substrate, (b) is the background without h-RBC, and (c) is the subtraction between (a) and (b). The data shown are the mean of spectra collected from five cells in each case. The acquisition time with each single cell was ~30 s with ~2 mW excitation. (C) Time- lapsed Raman spectra of trapped h-RBCs along with the background. Acquisition time for each spectra was 10 s with ~2 mW excitation. The presented spectra are the mean of the spectra from five h-RBCs. (D) Time-lapsed Raman spectra of a trapped RBC with a higher excitation power of ~5 mW over a duration of ~2 min. The spectra were recorded using 1200 lines/mm grating. Raman bands showing significant temporal changes are indicated by arrows. Also the baseline level is seen to increase with time.

from five healthy donors and five malaria patients is shown in Figs. 4(A)(a)–(c), respectively. One can see the significant improvement in SNR: ~34 dB as compared to ~22 dB for individual cell spectra.

It is worthwhile to note that although the blood samples collected from *P. vivax*-infected patients were having ~1 to 2% parasitized or infected cells (the level of parasitemia considered to be significant as per World Health Organization guidelines[30,31]), it is well known that apart from the fraction of red cells invaded by the parasites, a large fraction of nonparasitized cells may also have altered characteristics in malaria patients. Such changes may be directly induced by exo-antigens/chemicals released by the parasites[32–34] or dyserythropoiesis resulting from the

infection.[35,36] With the SNR available in the present study, significant changes in the Raman spectra were observed in ~30% of the red blood cells of the blood samples from malaria infected patients studied in the present experiment.

Apart from the prominent changes observed for methine hydrogen deformation doublet at 1210 and 1223 cm^{-1}, the spectra from m-m-RBCs show changes in Raman bands at 1366/ 1356 cm^{-1} (ν_4) and the spin marker bands in the region 1500 to 1700 cm^{-1}. In Table 1, we show the assignment of these Raman bands based on the work of Abe et al.[37] and Wood et al.[21]

In Fig. 5, we show a scatter plot of the intensities of the Raman bands at 1210 and 1223 cm^{-1}, 1356 and 1366 cm^{-1}, and 1546 and 1636 cm^{-1} for h-RBCs and m-m-RBCs. The left
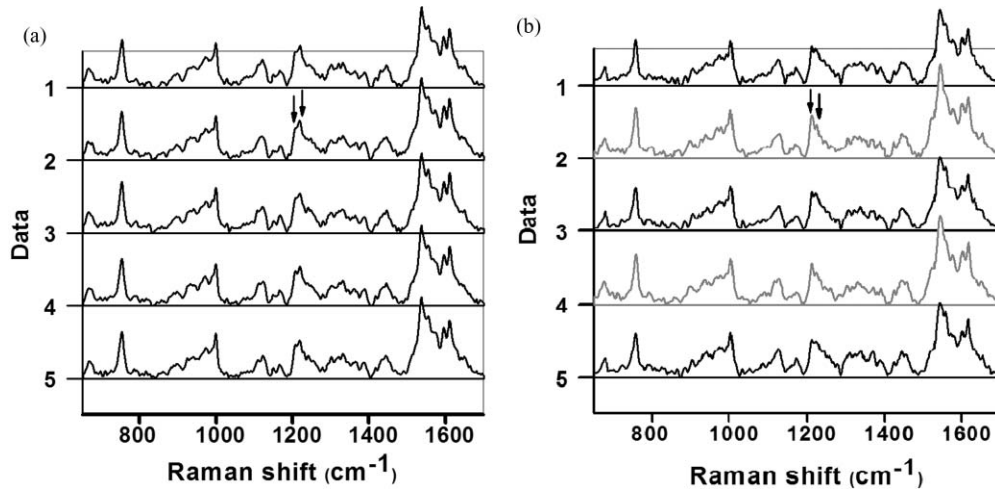
Fig. 3 Representative Raman spectra as collected from (a) h-RBCs and (b) m-RBCs. Each of the spectra were acquired over 30 s with ~2 mW of excitation at 785 nm. All of the spectra were smoothened using a Savitzky-Golay filter for removal of noise. The spectra from h-RBCs show nearly uniform spectral characteristics. However, the Raman spectra from a significant fraction of m-RBCs have characteristics different from that of the h-RBCs. The most noticeable changes in methine deformation bands at 1210 and 1223 cm^{-1} are indicated by arrows.

column shows the intensities of these bands in the mean Raman spectrum obtained from m-m-RBCs and h-RBCs. In the right column, the normalized intensities of the Raman bands for all h-RBCs and m-m-RBCs studied are presented to show inter- and intraclass scatter in data. Notably, the numbers presented in the scatter plots are the peak intensities of the relevant Raman
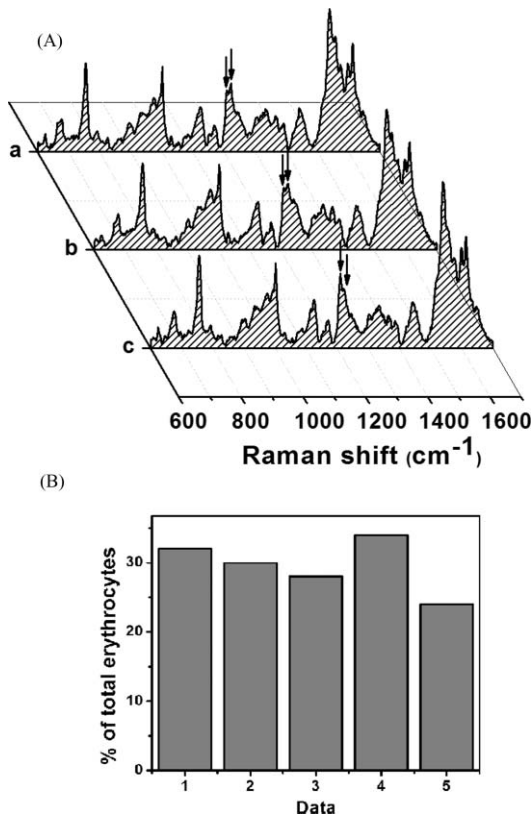

Fig. 4 (A) Mean Raman spectra of (a) h-RBCs, (b) nm-m-RBCs, and (c) m-m-RBCs. Spectra were recorded from 15 cells from each healthy donor and nearly 50 cells from each malaria patient. (B) Percentage of m-m-RBCs from each malaria patient.

bands. Since the Raman bands at 1210 cm^{-1}, 1223 cm^{-1} and 1356 cm^{-1}, 1366 cm^{-1} in Figs. 5(a) and 5(b), respectively, have well separated peaks, the peak intensities of these bands measured directly from the spectrum were used in the related scatter plots. However, the eight spin marker Raman bands in the region 1500 to 1700 cm^{-1} are closely spaced and strongly overlapped. The peak position of these bands cannot be determined directly from the spectra. In this case, multiple peak fitting was applied. The previous reports by Wood et al.[21,23] show that the Raman spectrum of RBCs is dominated by intracellular Hb and that Hb Raman spectrum in the range 1500 to 1700 cm^{-1} has eight bands that can be denoted as ν_{38}, ν_{11}, ν_{19}, ν_{37}, $\nu(C=C)_{vinyl}$, $\nu(C=C)_{vinyl}$, ν_{10}, and Amide I.[21,23] Eight Lorentzian peaks allowed independent variation in terms of intensity, width and position were used to obtain the best fit profile to the experimental data. It can be seen that the fitted profile approximate quite well with the observed data. Therefore, the peak intensities of the fitted Lorentzian profiles were used in the related scatter plot.

The ratio between the Raman bands at 1210 and 1223 cm^{-1} in the mean spectrum from m-m-RBCs were observed to have an average value of ~1:0.79, different from the value of 1:1.13 observed in the mean spectrum from h-RBCs [Fig. 5(a)]. The intensities of the Raman bands for each h-RBCs and m-m-RBCs are shown in the right column. The relative intensities of the Raman bands can be clearly seen to be well distinguishable for the h-RBCs and m-m-RBCs. Further, for mean Raman spectra from m-m-RBCs, we also observed partial shifting of the Raman band at ~1366 to 1356 cm^{-1} in comparison to h-RBCs mean spectra [Fig. 5(b)]. The intensities of 1356 and 1366 cm^{-1} Raman bands for each h-RBCs and m-m-RBCs are shown in the right column. For spin marker bands in the 1500 to 1700 cm^{-1} region, major changes can be seen for the 1546 cm^{-1} peak (ν_{11}) and 1636/1633 cm^{-1} peak (ν_{10}) and, therefore, intensity for these peaks for each h-RBCs and m-m-RBCs are shown in the right column of Figs. 5(c) and 5(d). While intensity of the peak at 1546 cm^{-1} is found to be enhanced in the case of m-m-RBCs with respect to that for h-RBCs, the opposite can be seen for the Raman band at 1636 cm^{-1}. The 1636 cm^{-1} band for h-RBCs was

Table 1 Assignment and spectral position (cm^{-1}) of the Hb Raman bands showing significant changes between h-RBC and m-m-RBC. For comparison, bands observed by Wood et al. (Ref. 21) are also shown.

Band assignment	Local coordinates	Hb band position (cm^{-1}) in m-m-RBC	Hb band position (cm^{-1}) in h-RBC	Deoxy-Hb band position (cm^{-1}) (Ref. 14)	Oxy-Hb band position (cm^{-1}) (Ref. 14)
$\nu_5 + \nu_{18}$	$\delta(C_mH)$	1210	1210	1213	1212
ν_{13} or ν_{42}	$\delta(C_mH)$	1223	1223	1223	1226
ν_{42}	$\delta(C_mH)$	1245	1245	1248	1248
ν_4	$\nu(\text{pyr half-ring})_{sym}$	1356/1366	1366	1356	1371
ν_{11}	$\nu(C_\beta C_\beta)$	1546	1546	1548	1547
ν_{10}	$\nu(C_\alpha C_m)_{asym}$	1633	1636	Absent	1639

also found to be shifted to 1633 cm^{-1} in the spectra from m-m-RBCs. However, this shift is below the resolution of the set-up (6 cm^{-1}) and thus not significant. The differences in intensity ratios for the Raman bands between h-RBCs and m-m-RBCs were found to be significant to a p value of <0.05 for all cases (a–c).

The available Raman data of model porphyrin compounds[37,38] suggests that the abovementioned changes can be attributed to changes in the oxygenation status of the intra-erythrocytic Hb. The most striking change in the spectra recorded from m-m-RBCs is the change in the ratio of the intensities of the 1210 and 1223 cm^{-1} peaks. While Salmaso et al.[39] have assigned the 1223 cm^{-1} band to ν_{13} and the band at 1210 cm^{-1} to $\nu_5 + \nu_8$, the 1223 cm^{-1} has also been assigned to ν_{42}.[38] These modes are associated with C-H in plane vibrations of methine hydrogen. Proximity to the protein subunits influences the deformation angle and consequently a change in intensities between the planar oxygenated (oxy-Hb) and nonplanar deoxygenated (deoxy-Hb) Hb structure. It is known that the doublet located at 1245 and 1223 cm^{-1} in the spectra of low spin heme (oxy-Hb) get shifted to 1223 and 1210 cm^{-1} in the spectra of high spin heme (deoxy-Hb).[21,24] Studies carried out on RBCs subjected to periodic oxygenation and de-oxygenation cycles have also revealed significant enhancement of the intensity of the 1210 cm^{-1} band for deoxy-Hb.[21] Therefore, observed elevated intensity at 1210 cm^{-1} for m-m-RBCs over h-RBCs suggests a complete or partly deoxygenated state of a significant fraction ($\sim$30%) of the m-RBCs in *P. vivax*-infected blood samples.

It is pertinent to note that the RBCs used in our experiments were collected by venipuncture and will therefore be initially in a deoxygenated state. However, for normal functional state of Hb, these should almost completely get transformed into an oxygenated condition upon exposure to atmospheric oxygen.[23] The Raman signatures of m-m-RBCs, on the other hand, suggest that a significant number of red cells from blood samples of malaria infected patients were only partially oxygenated or remained deoxygenated even after exposure to atmospheric oxygen. This could be further verified by studying the relative intensities of the bands at 1366 and 1356 cm^{-1}. The bands appearing between 1366 cm^{-1} (oxy-Hb) and 1356 cm^{-1} (deoxy-Hb) assigned to local co-ordinate ν_4 (Refs. 24, 37, and 40) involve pyrrole half ring stretching vibration and are known as oxidation

state markers. The oxygen molecule upon binding to deoxy-Hb withdraws an electron from the ferrous [Fe(II)] ion leaving the metal in a low spin ferric [Fe(III)] state in oxy-Hb and results in an increase in vibrational wavenumber of the ν_4 mode.[23,24] We observed partial suppression of the band at 1366 cm^{-1} for m-m-RBCs and a corresponding enhancement of the band at 1356 cm^{-1}, suggesting a partially de-oxygenated state of the cells.

The bands in the region between 1500 to 1700 cm^{-1} are known to serve as spin state markers. The normal mode at 1546 cm^{-1} (ν_{11}) primarily consists of C_β–C_β bond stretching, which is strongly influenced by the conformational transitions and, hence, show significant change in intensity between the planar oxy-Hb and nonplanar deoxy-Hb structures and is known to be the most intense band in the deoxygenated form.[21,41] In our study, we also observed significant enhancement in intensity at this band for m-m-RBCs. We also observed a partial suppression of the ν_{10} band (1636 cm^{-1}) for m-m-RBCs, which is also suggestive of the presence of partially oxygenated Hb inside the cells.[21]

To summarize, the observed changes in the Raman bands in m-m-RBCs suggest a reduction of Hb-oxygen affinity, which are consistent with the results of a previous study on *P. berghei* infected mice.[42] It is known that metabolic acidosis, a common complication of malaria, can cause a lowering of blood pH (down to $\sim$7.2 to 7.0) in malaria patients.[2,43] This can affect the oxygen affinity of Hb via the Bohr effect. However, in our study, RBCs collected from malaria patients and healthy persons were suspended in an identical phosphate buffer solution ($pH \sim 7.4$) and stabilized for $\sim$1 h before recording the Raman spectra. Therefore, a pH change induced shift of oxygen dissociation curve cannot account for the observed spectral changes. Another potential cause that can effect an altered Hb-oxygen affinity is the intracellular concentration of 2,3-Diphosphoglycerate (2,3-DPG), an important metabolite in RBCs, involved in the stabilization of the deoxy-form of Hb. Also, dyserythropoiesis or ineffective erythropoiesis has been reported in adults with *P. vivax* malaria, which correlated well with the severity of the anemic condition.[35] Such dyserythropoeisis may often consist of megaloblastosis,[36,44] which has been known to be associated with an increased level of 2,3-DPG and consequent decrease of Hb-oxygen affinity.[45]
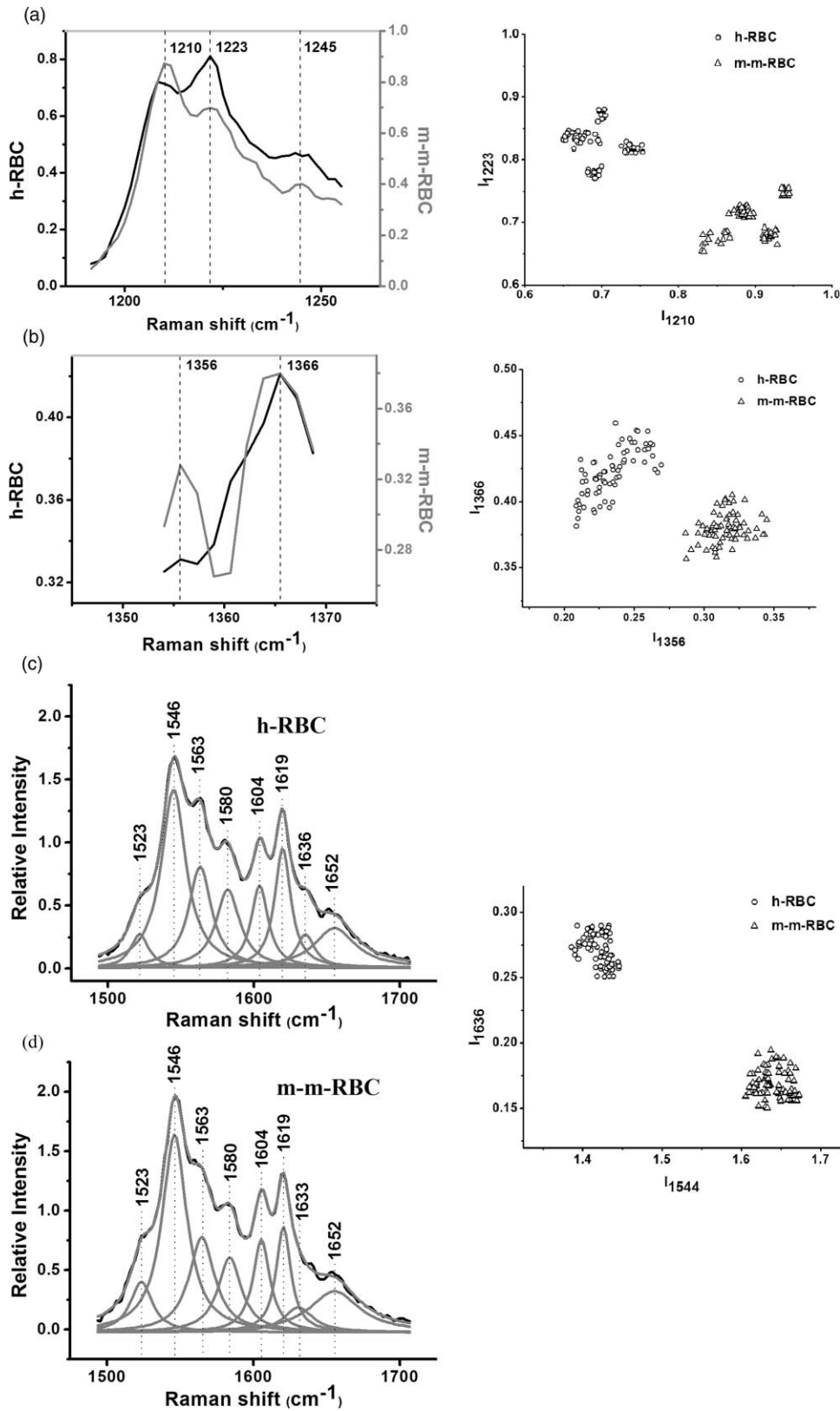
Fig. 5 Raman bands showing significant intensity differences in the spectra recorded from m-m-RBCs over that recorded from h-RBCs. Left column: (a) and (b) Relative intensity of bands in the mean Raman spectra of h-RBCs (dark line) and the mean spectra for m-m-RBCs (faded line). The mean Raman spectra (dark line) for ~1500 to 1700 cm^{-1} region and the fitted peaks for (c) h-RBCs and (d) m-m-RBCs are shown. Right column: Scatter plot showing intensities of the Raman bands for all of the h-RBCs and m-m-RBCs studied. It can be seen that the Raman band intensities for h-RBCs and m-m-RBCs are well separated.

4 Conclusion

Employment of Raman optical tweezers facilitated means for single-cell level evaluation of the oxygenation state of the RBCs from malaria patients. The Raman spectroscopic studies carried out on optically trapped red blood cells collected from blood samples of healthy volunteers (h-RBCs) and from patients suffering from the *P. vivax* infection (m-RBCs) reveal that a significant fraction of m-RBCs produced Raman spectra with altered characteristics relative to h-RBCs. The observed spectral changes suggest a reduced oxygen-affinity or right shifting of the oxygen-dissociation curve for the intracellular hemoglobin with respect to its normal functional state. Recently, *P. vivax* malaria has been reported to cause a severe anemic condition and acute respiratory distress syndrome in patients, which may result in a hospital stay and even mortality.[46,47] Raman spectroscopic study of m-RBCs in blood sample of *P. vivax*-infected patients may provide a useful means for estimation of complication that may result from altered oxygen loading capability of RBCs in malaria patients.

References

1. S. Rogerson, "What is the relationship between haptoglobin, malaria, and anaemia," *PLoS Med.* **3**, 593–594 (2006).
2. I. W. Sherman, *Malaria: Parasite Biology, Pathogenesis and Protection*, American Society for Microbiology, Washington, DC (1998).
3. R. N. Price, J. A. Simpson, F. Nosten, C. Luxemburger, L. Hkirjaroen, F. ter Kuile, T. Chongsuphajaisiddhi, and N. J. White, "Factors contributing to anemia after uncomplicated falciparum malaria," *Am. J. Trop. Med. Hyg.* **65**, 614–622 (2001).
4. S. Suresh, J. Spatz, J. P. Mills, A. Micoulet, M. Dao, C. T. Lim, M. Beil, and T. Seufferlein, "Connections between single-cell biomechanics and human disease states: gastrointestinal cancer and malaria," *Acta Biomater.* **1**, 15–30 (2005).
5. S. K. Mohanty, A. Uppal, and P. K. Gupta, "Self-rotation of red blood cells in optical tweezers: prospects for high throughput malaria diagnosis," *Biotechnol. Lett.* **26**, 971–974 (2004).
6. J. A. Dharmadhikari, S. Roy, A. K. Dharmadhikari, S. Sharma, and D. Mathur, "Naturally occurring, optically driven, cellular rotor," *Appl. Phys. Lett.* **85**, 6048–6050 (2004).
7. S. K. Mohanty, K. S. Mohanty, and P. K. Gupta, "Dynamics of interaction of RBC with optical tweezers," *Opt. Express* **13**, 4745–4751 (2005).
8. M. Khan, S. K. Mohanty, and A. K. Sood, "Optically-driven red blood cell rotor in linearly polarized laser tweezers," *Pramana* **65**, 777–786 (2005).
9. K. Mohanty, S. Mohanty, S. Monajembashi, and K. O. Greulich, "Orientation of erythrocytes in optical trap revealed by confocal fluorescence microscopy," *J. Biomed. Opt.* **12**, 060506 (2007).
10. S. K. Mohanty, A. Uppal, and P. K. Gupta, "Optofluidic stretching of RBCs using single optical tweezers," *J. Biophoton.* **1**, 522–525 (2008).
11. K. Bambardekar, A. K. Dharmadhikari, J. A. Dharmadhikari, D. Mathur, and S. Sharma, "Measuring erythrocyte deformability with fluorescence, fluid forces, and optical trapping," *J. Biomed. Opt.* **13**, 064021 (2008).
12. V. Saraogi, P. Padmapriya, A. Paul, U. S. Tatu, and V. Natarajan, "Change in spectrum of Brownian fluctuations of optically trapped red blood cells due to malarial infection," *J. Biomed. Opt.* **15**, 037003 (2010).
13. C. Brémard, J. J. Girerd, P. Kowalewski, J. C. Merlin, and S. Moreau, "Spectroscopic investigations of malaria pigment," *Appl. Spectrosc.* **47**, 1837–1842 (1993).
14. B. R. Wood, S. J. Langford, B. M. Cooke, J. Lim, F. K. Glenister, M. Duriska, J. K. Unthank, and D. McNaughton, "Resonance Raman spectroscopy reveals new insight into the electronic structure of β-hematin and malaria pigment," *J. Am. Chem. Soc.* **126**, 9233–9239 (2004).
15. C. W. Ong, Z. X. Shen, K. K. H. Ang, U. A. K Kara, and S. H. Tang, "Raman microspectroscopy of normal erythrocytes and Plasmodium berghei-infected erythrocytes," *Appl. Spectrosc.* **56**, 1126–1131 (2002).
16. B. R. Wood, J. L. Steven, B. M. Cooke, F. K. Glenister, J. Lim, and D. McNaughton, "Raman imaging of hemozoin within the food vacuole of *Plasmodium falciparum* trophozoites," *FEBS Lett.* **554**, 247–252 (2003).
17. D. V. Petrov, "Raman spectroscopy of optically trapped particles," *J. Opt. A: Pure Appl. Opt.* **9**, S139–S156 (2007).
18. A. Min, L. Jun-Xian, H. Shu-Shi, W. Gui-Wen, C. Xiu-Li, C. Zhi-Cheng, and Y. Hui-Lu, "Application and progress of Raman tweezers in single cells," *Chin. J. Anal. Chem.* **37**, 758–763 (2009).
19. 2008 Undergraduate Summer Research Program in Modern Optics and Optical Materials: Detection of nanosize biological threats. Retrieved 14 December, 2009, from University of Arkansas Web site: http://www.uark.edu/depts/physics/reu05/proj-4.html; K. Ramser, C. Fant, and M. Kall, "Importance of substrate and photo-induced effects in Raman spectroscopy of single functional erythrocytes," *J. Biomed. Opt.* **8**, 173–178 (2003).
20. C. A. Lieber and A. Mahadevan-Jansen, "Automated method for subtraction of fluorescence from biological raman spectra," *Appl. Spectrosc.* **57**, 1363–1367 (2003).
21. B. R. Wood, P. Caspers, G. J. Puppels, S. Pandiancherri, and D. McNaughton, "Resonance Raman spectroscopy of red blood cells using near infrared excitation," *Anal. Bioanal. Chem.* **387**, 1691–1703 (2007).
22. B. R. Wood, L. Hammer, L. Davis, and D. McNaughton, "Raman microspectroscopy and imaging provides insights into heme aggregation and denaturation within human erythrocytes," *J. Biomed. Opt.* **10**, 014005 (2005).
23. B. R. Wood and D. McNaughton, "Raman excitation wavelength investigation of single red blood cells *in vivo*," *J. Raman. Spectrosc.* **33**, 517–523 (2002).
24. B. R. Wood, B. Tait, and D. McNaughton, "Micro-Raman characterisation of the R to T state transition of haemoglobin within a single living erythrocyte," *Biochim. Biophys. Acta* **1539**, 58–70 (2001).
25. Y. K. Park, M. Diez-Silva, G. Popescu, G. Lykotrafitis, W. Choi, M. S. Feld, and S. Suresh, "Refractive index maps and membrane dynamics of human red blood cells parasitized by Plasmodium falciparum," *Proc. Natl. Acad. Sci. U.S.A.* **105**, 13730–13735 (2008).
26. A. Trommler, D. Gingell, and H. Wolf, "Red blood cells experience electrostatic repulsion but make molecular adhesions with glass," *Biophys. J.* **48**, 835–841 (1985).
27. K. Ramser, K. Logg, M. Goksor, J. Enger, M. Kall, and D. Hanstorp, "Resonance Raman spectroscopy of optically trapped functional erythrocytes," *J. Biomed. Opt.* **9**, 593–600 (2004).
28. E. J. G. Peterman, F. Gittes, and C. F. Schmidt, "Laser-induced heating in optical traps," *Biophys. J.* **84**, 1308–1316 (2003).
29. R. Dasgupta, S. Ahlawat, R. S. Verma, A. Uppal, and P. K. Gupta, "Hemoglobin degradation in human erythrocytes with long duration near infrared laser exposure in Raman optical tweezers," *J. Biomed. Opt.* **15**, 055009 (2010).
30. "Determination of Parasitemia," retrieved 8 August 2010 from http://www.med-chem.com/procedures/DetofPara.pdf
31. H. Löffler, J. Rastetter, and T. Haferlach, *Atlas of clinical hematology*, pp. 401, Springer, New York (2005).
32. K. M. Naumanna, G. L. Jonesb, A. Saulb, and R. Smith, "A Plasmodium falciparum exo-antigen alters erythrocyte membrane deformability," *FEBS Lett.* **292**, 95–97 (1991).
33. A. M. Dondorp, P. A. Kager, J. Vreeken, and N. J. White, "Abnormal blood flow and red blood cell deformability in severe malaria," *Parasitology Today* **16**, 228–232 (2000).
34. F. Nuchsongsin, K. Chotivanich, P. Charunwatthana, O. S. Fausta, D. Taramelli, N. P. Day, N. J. White, and A. M. Dondorp, "Effects of

malaria heme products on red blood cell deformability," *Am. J. Trop. Med. Hyg.* **77**, 617–622 (2007).

35. S. N. Wickramasinghe, S. Looareesuwan, B. Nagachinta, and N. J. White, "Dyserythropoiesis and ineffective erythropoiesis in Plasmodium vivax malaria," *Br. J. Haematol.* **72**, 91–99 (1989).

36. P. Pradhan, "Malarial anaemia and nitric oxide induced megaloblastic anaemia: a review on the causes of malarial anaemia," *J. Vector Borne Diseases* **46**, 100–108 (2009).

37. M. Abe, T. Kitagawa, and Y. Kyogoku, "Resonance Raman spectra of octaethylporphyrinato-Ni(II) and meso-deuterated and ^{15}N substituted derivatives. II. A normal coordinate analysis," *J. Chem. Phys.* **69** 4526–4534 (1978).

38. S. Hu, K. M. Smith, and T. G. Spiro, "Assignment of protoheme resonance Raman spectrum by heme labeling in myoglobin," *J. Am Chem. Soc.* **118**, 12638–12646 (1996).

39. B. L. N. Salmaso, G. J. Puppels, P. J. Caspers, R. Floris, R. Wever, and J. Greve, "Resonance Raman microspectroscopic characterization of eosinophil peroxidase in human eosinophilic granulocytes," *Biophys J.* **67**, 436–446 (1994).

40. T. Yamamoto and G. Palmer, "The valence and spin state of iron in oxyhemoglobin as inferred from resonance Raman spectroscopy," *J. Biol. Chem.* **248**, 5211–5213 (1973).

41. M. Forster, R. E. Hester, B. Cartling, and R. Wilbrandt, "Continuous flow-resonance Raman spectroscopy of an intermediate redox state of cytochrome c," *Biophys. J.* **38**, 111–116 (1982).

42. F. Palaceck, M. Palacekova, and D M Aviado, "Pathologic physiology and chemotherapy of Plasmodium berghei: II. Oxyhemoglobin dissociation curve in mice infected with chloroquine-sensitive and resistant strains," *Exp. Parasitol.* **21**, 16–30 (1967).

43. P. Sasi, S. P. Burns, C. Waruiru, M. English, C. L. Hobson, C. G. King, M. Mosobo, J. S. Beech, R. A. Iles, B. J. Boucher, and R. D. Cohen, "Metabolic acidosis and other determinants of hemoglobin-oxygen dissociation in severe childhood Plasmodium falciparum Malaria," *Am. J. Trop. Med. Hyg.* **77**, 256–260 (2007).

44. S. N. Wickramasinghe and S. H. Abdalla, "Blood and bone marrow changes in malaria," *Baillièrès Clinical Haematol.* **13**, 277–299 (2000).

45. F. J. Fernandes-Costa, R. Green, and J. D. Torrance, "Increased erythrocytic diphosphoglycerate in megaloblastic anaemia. A compensatory mechanism?," *S. Afr. Med. J.* **53**, 709–712 (1978).

46. R. N. Price, E. Tjitra, C. A. Guerra, S. Yeung, N. J. White, and N. M. Anstey, "Vivax malaria: neglected and not benign," *Am. J. Trop. Med. Hyg.* **77**(6 suppl), 79–87 (2007).

47. A. Aparecida, M. Fernandes, L. José de Moura Carvalho, G. M. Zanini, A. M. R. da Silva Ventura, J. M. de Souza, P. M. Cotias, I. L. Da Silva Filho, and C. T. Daniel Ribeiro, "Similar Cytokine responses and degrees of anemia in patients with *Plasmodium falciparum* and *Plasmodium vivax* infections in the Brazilian Amazon region," *Clin. Vaccine Immunol.* **15**, 650–658 (2008).